Proceedings of 15th IOE Graduate Conference
Peer Reviewed
Year: 2024 Month: May Volume: 15
ISSN: 2350-8914 (Online), 2350-8906 (Print)

A Current-Controller for Integration Hybrid Microgrid in Existing System

Supriya Pandeya [a], Menuka Karki [b]

[a, b] *Department of Electrical Engineering, Pashimanchal Campus, IOE, Tribhuvan University, Nepal*
[a] supriya.762540@pasc.tu.edu.np, [b] menaka.karki@pasc.tu.edu.np

Abstract
The growing demand for clean energy has led to the emergence of hybrid microgrids, integrating both AC and DC systems. Managing disturbances and uncertainties while enhancing performance remains a challenge. This study proposes a control strategy for hybrid microgrids, including single-phase controller design and simulation. A simplified dq controller is introduced to improve dynamic response without increasing complexity. Additionally, a three-phase grid-connected inverter (3-φ GCI) is simulated to meet IEEE requirements for total harmonic distortion (THD). The control scheme utilizes unipolar switching in the dq axis theory with sinusoidal pulse width modulation (SPWM) for independent control of active and reactive grid currents. The project employs MATLAB to simulate and develop the hybrid microgrid system, integrating photovoltaic panels, battery storage, wind generation, and utility grid integration. A comprehensive controller supports both single-phase and three-phase systems, enabling analysis of grid interactions, renewable energy generation, and controller performance metrics. The study advances understanding of hybrid microgrid dynamics and supports the development of sustainable energy systems.

Keywords
phase lock loop, d-q, synchronous reference frame, MATLAB, LCL filter, PWM generator

1. Introduction

The increasing integration of renewable energy sources and distributed generations (DGs) into power distribution networks has propelled the emergence of microgrids as a vital solution. These microgrids provide a controlled environment for various DGs, local loads, and energy storage systems to operate seamlessly in both grid-connected and is landing modes. While AC microgrids, which connect to the utility grid at the point of common coupling (PCC), have garnered significant attention, the rise of solar photovoltaics (PV), energy storage systems, and DC loads like data centers and LED lighting has sparked interest in DC microgrids [1].

Efficient management of microgrids relies on effective control strategies, with droop-based hierarchical strategies proving prominent. These strategies, effective for both AC and DC microgrids, streamline control and enhance power quality. With the increasing integration of DC sources and loads within AC-dominant networks, hybrid AC/DC microgrids have emerged as promising avenues for future power distribution systems [1].

As per Annual Report of NEA 2023, The Government of Nepal (GoN) has embarked on a significant initiative, the Grid Solar Energy and Energy Efficiency Project (GSEEP). This project is primarily financed by a credit from the World Bank (WB), amounting to 130 million USD, under IDA Credit No. 5566-NP (Project ID P146344). In addition to this, the GoN has also contributed 8 million USD as counter financing. The GSEEP aims to harness solar energy and enhance energy efficiency in Nepal, marking a crucial step towards achieving the country's sustainable development goals.This demands more advancement and research in the field of controller for AC and DC integration as Solar or most renewable sources are DC in nature [2]. In hybrid microgrid operation,bidirectional interlinking-converters (BICs) play a crucial role in facilitating efficient power management and maintaining power quality. Control strategies for BICs fall into centralized and decentralized categories. Decentralized methods, such as universal AC/DC droop control, provide reliable proportional power sharing without extensive communication [3].

The traditional definition of reactive power in single-phase or three-phase circuits is based on the average value concept for sinusoidal voltage and current waveforms in steady states. However, the instantaneous reactive power in three-phase circuits is defined based on the instantaneous value concept for arbitrary voltage and current waveforms, including transient states [4]. A novel instantaneous reactive power compensator, which consists of switching devices and practically eliminates the need for energy storage components, is suggested [5]. Grid integration of DC power sources, such as solar photovoltaic (PV) systems, presents several challenges. These include issues related to power quality, angular and voltage stability, reactive power support [5], and fault ride-through capability. The intermittent nature of renewable energy sources also poses operational and technical challenges, hampering network reliability and stability.

Moreover, BICs in hybrid microgrids offer AC/DC voltage support during main voltage source failures, contributing to enhanced system resilience [6]. Recently, the concept of community microgrids has emerged, combining the benefits of AC and DC microgrids for improved reliability and economic performance [7].

However, detailed formulations for implementing and coordinating community microgrids remain limited [6]. To

address this gap, this paper introduces a novel three-level hierarchical coordination strategy inspired by droop control [6]. This strategy extends to encompass multiple AC and/or DC microgrids within a community microgrid, regulating power exchanges during islanded and grid-connected modes [8].As the field of hybrid microgrid control evolves, addressing the interplay between hybrid AC/DC microgrids, BIC control strategies, and voltage support mechanisms remains a dynamic challenge . Hierarchical control approaches aim to optimize power management, ensure grid stability, and facilitate efficient resource utilization, advancing resilient and sustainable power distribution networks [3].

2. Methodology

A hybrid AC/DC microgrid system with various distributed generators (DGs), energy storage systems (ESSs), and loads coupled to appropriate AC and DC subgrids is depicted in Figure 1. The Interlinking Converter (ILC) makes it easier for these subgrids to support and interchange power. Grid-connected mode allows power support from the utility grid, while plug-and-play functionality allows autonomous power sharing using DG droop management.

PV with BESS: The MATLAB/EMTDC simulation makes use of a solar PV library model, which necessitates the provision of cell temperature and irradiance data. Series and parallel configurations of solar modules and cells are possible based on the voltage and power needs. For the sake of our DC-AC hybrid microgrid simulation, the PV array acts as a reference. The solar PV properties are validated by characteristic curves at different irradiances. The parameters used in the PV array simulations are shown in Table 1.

The MATLAB/EMTDC embedded battery library model is used by the system. To extract as much electricity as possible from solar PV, a DC-DC buck converter regulates it.Battery charging and discharging circuits are regulated to maintain the DC link voltage within acceptable bounds.The grid-tied rectifier delivers power in the absence of solar PV and batteries.

The battery's state of charge determines how much to charge and how much to discharge (SOC). SOC is kept between 30% and 90% to prevent overcharging and deep discharging. The SOC 90% and PV power (PPV) > load power (PLoad) = charging are the components of SOC-based activities. Discharge if SOC 30% and PPV PLoad. Load shedding will happen if SOC is 30%, PPV is load, and the grid is offline. Solar PV systems that have a SOC 90% and a PPV > load will disconnect. Wind Generator: As part of distributed generating, compact generators are connected to the distribution level, close to end users. To illustrate this concept, an assortment of distributed generators (DGs) in an AC subgrid, including synchronous, wind, and solar generators, can be employed. The suggested model makes use of a wind generator.

This wind turbine has a doubly-fed wound-rotor induction generator and varies in speed. With a frequency of 50 Hz and a line voltage of 0.6 kV, the generator has a 100 kVA rating. The generator's input torque (T=0.25 PU) represents the wind turbine. Reactive power can be given to the machine via the rotor by means of power electronics.

This setup allows for the efficient conversion and filtering of DC power for use in an AC grid. The LCL filter is a crucial component that ensures the quality of the power fed into the grid, minimizing harmonic distortion and improving overall system performance. The exact design and control of each component can vary depending on the specific requirements of the system.

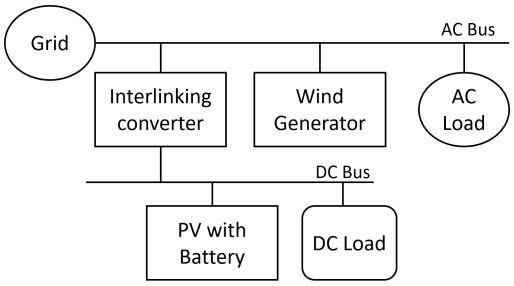

Figure 1: Block Diagram of Proposed Hybrid Microgrid

Utility: For the validation of proposed model, Utility is modelled. A three phase AC source is considered which is connected to the transformer and then to Pi circuit. Specification of all are mentioned in the model.

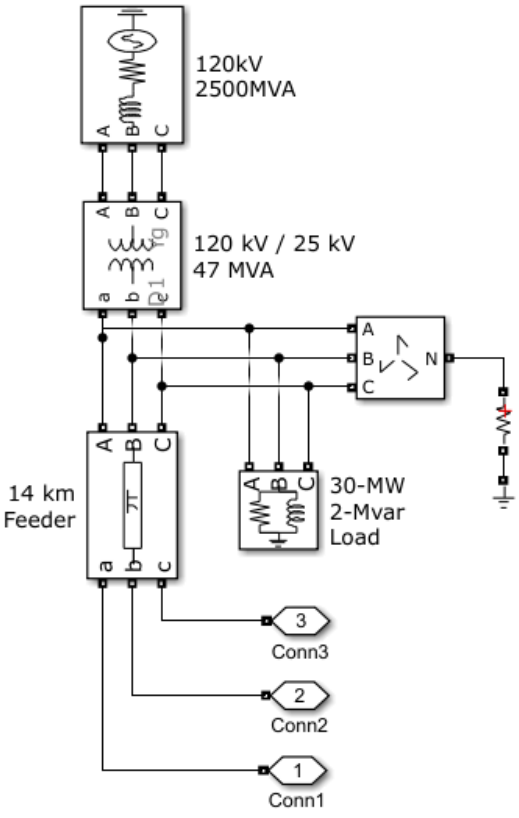

Figure 2: Utility

2.1 Topology of ILC

The following definitions are given for each variable: Rn and Ln are the nominal equivalent resistance and filter inductance; Cn is the filter capacitor; Ps and Qs are the transmission power of the ILC. Uabc and iabc are the converter voltage and current; Eabc is the AC bus voltage; idc and Udc are the DC side current and voltage of the converter.

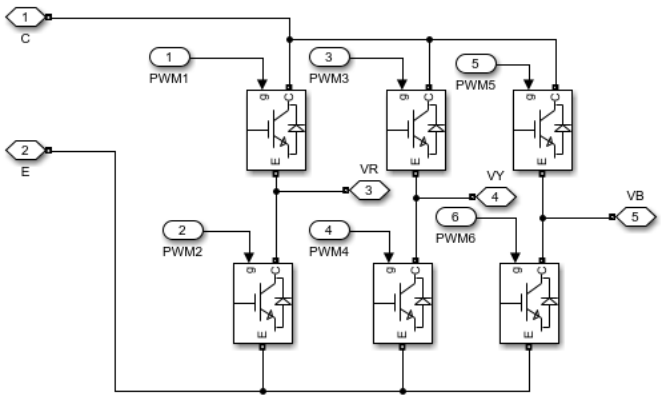

Figure 3: Topology of Interlinking Converter

2.2 Design of LCL

LCL filter is used to interconnect inverter with the grid in this design. As an inverter is based on switching devices and gating signals in the form of pulses must be provided for the switches, the output current can contain significant harmonic disturbances with tend to reduce power quality. The criteria for calculating the values of the components is presented below. All the calculations are carried out using per phase circuit. The inverter side inductor is sized as, Where, Li is the inverter side inductor per phase, fs is the switching frequency of the inverter = 30 kHz, $V_{\text{DC Link}}$ = 750 V, and ΔI_L is the ripple current of the inductor, which is chosen to be 10% of the phase current and can be computed using (7).

Where, P is nominal power of the system per phase = 200W Vph(grid) is the single-phase voltage of grid = 230V. After substituting these values, it is found that, Li = 13 mH. (9) $V_{\text{DC Link}}$ = 750 V, and ΔI_L is the ripple current of the inductor, which is chosen to be 10% of the phase current and can be computed using (7).

The obtained per phase capacitance for the filter is, Cf = 0.6uF Per, a damping resistor in series with the LCL filter capacitor should be added to increase the performance of the filter. This results in fo = 2943 Hz, and the value of damping resistor needed is 30 ohms per phase. However, in the simulation, a lower value is used.

$$Q = \frac{V^2}{\left(\frac{1}{2\pi f C}\right)} \tag{1}$$

Where, Q is reactive power f is frequency, C is the capacitance of the capacitor used as a filter, V is the voltage of the grid, Using equation (1), the value of capacitance is obtained. After that, value of both inductors is obtained. To gain the value of the inductor connected to the inverter side(L1) maximum permissible ripple current is set. Based upon the review, the current ripple is limited to 20% and the value of the inductor is gained. Inductor is given by;

$$L1 = \frac{V_{dc}}{4 f_{sw} \Delta I_{pp_{max}}} \tag{2}$$

Where, Vdc is DC side voltage, Fsw is switching frequency. With aid of equation (2), value of L1 is gained and this value is 4.06Mh. To calculate the value of the inductor connected on the grid side maximum voltage drop is limited to the 10% of rated capacity. The inductor of grid side is obtained as 4.85Mh.

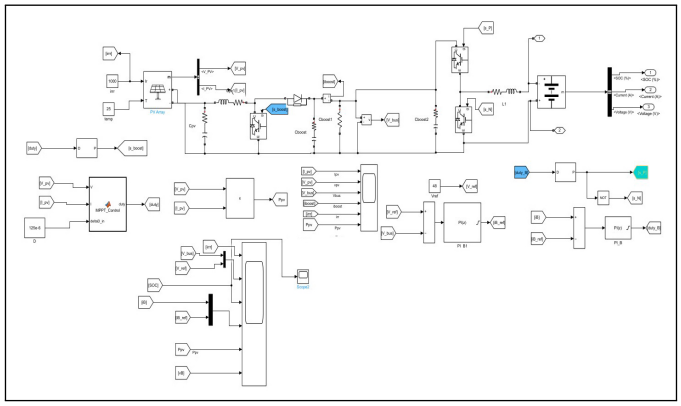

Figure 4: AC and DC source with Converter in MATLAB/SIMULINK

After the selection of inductors and capacitor for the filter, verification is done, which depends upon resonance frequency. It is found that the obtained resonance frequency is greater than 10 times of grid frequency and less than 0.5 times the switching frequency. Hence it is verified that the nominated value of the capacitor and inductors are suitable for the proposed single-phase model

2.3 Phase Loop Lock

Phase Loop Lock is used when it is required to send the current to the grid the then PLL is opted to generate reference current. To control the active power, PLL generates current in phase with the source voltage, and for the reactive power control it generates current having a phase difference with the main current. Then PLL of the model developed in which output of grid is provided to remove harmonics. [9]

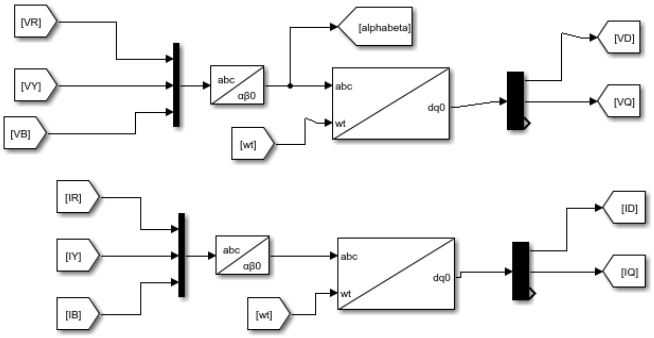

Figure 5: Phase Lock Loop

2.4 Synchronous D-Q Reference Frame

A key challenge in using proportional-integral (PI) controllers to manage time-varying signals such as sinusoidal currents and voltages is that these controllers cannot achieve zero steady-state error. To circumvent this issue, the synchronous

reference frame can be employed to depict time-varying signals as DC signals [10]. The underlying principle is that a phasor rotating at an angular velocity ω appears stationary relative to a reference phasor rotating at the same angular velocity ω in the same direction.

$$\vec{A} = A \cdot e^{j(\omega\ t+\phi)} \tag{1}$$

- $\vec{A}$ is the phasor
- A is the magnitude of the phasor
- ω is the angular velocity
- t is the time
- ϕ is the phase

The transformation from a three-phase natural frame to the Stationary Reference Frame, also known as the Clarke transformation, is executed for time-varying three-phase signals. The transformation from the Stationary Reference Frame to the Synchronous Reference Frame is crucial for effective signal control. While a three-phase signal can be converted into two quadrature phases, these signals still rotate at an angular frequency similar to the initial three-phase vectors. Proportional-integral (PI) controllers cannot be applied to these signals as they won't produce zero steady-state error.

The transformation matrix as represented by equation (9), is then applied. Within the domain, the reference frames rotate at the same angular frequency as the input signals, resulting in no relative motion between the vectors and the references. Consequently, these vectors are perceived as DC quantities. This characteristic allows PI controllers to effectively regulate these signals. The methodology described has been implemented using a Simulink block. The conversion of a three-phase signal into two phases that are orthogonal to each other is possible. However, these two signals continue to rotate at an angular frequency similar to the original three-phase vectors. As a result, PI controllers cannot be used with these signals because they will not yield a zero steady-state error.

The dq transformation matrix is represented as follows:

$$\begin{bmatrix} X_d \\ X_q \end{bmatrix} = \begin{bmatrix} \cos\theta & -\sin\theta \\ \sin\theta & \cos\theta \end{bmatrix} \begin{bmatrix} X_\alpha \\ X_\beta \end{bmatrix} \tag{2}$$

In the dq reference frames, there is no relative motion between the vectors and the references since they rotate at the same angular frequency as the input $\alpha\beta$ signals. As a result, these vectors appear as DC quantities, allowing PI controllers to effectively control these signals [9].

The Simulink block used to generate orthogonal signals for the single-phase case of synchronous frame transformation is based on the Second Order Generalized Integrator (SOGI) technique.

2.5 Control System

The control system for the grid-connected operation of the inverter is implemented using cascaded control loop structures. The inverter primarily operates in a current-controlled mode. This mode is managed by the inner control loop, which is responsible for implementing the current control. The outer loop, on the other hand, is responsible for power control. It provides the capability to control active and reactive power. This control can be achieved either directly through given reference values or indirectly through the regulation of the DC link voltage. In this setup, the DC link voltage regulation serves as a mechanism for controlling the active power output of the inverter. This method offers a degree of flexibility and adaptability, making it suitable for a variety of applications beyond photovoltaic systems. It allows for precise control of power output, ensuring efficient operation and optimal performance of the inverter when connected to the grid. This control scheme aims to regulate the current output to the grid based on the power demand specified by the outer control loop. The current control loop generates a reference voltage signal, which is compared with a triangular carrier waveform to produce the PWM signals for IGBT switching. These signals shape the required inverter output voltage waveform.

The control is executed in the dq reference frame to prevent non-zero steady-state error. However, to ensure that the dq frame-transformed signals remain in sync with the grid, a phase-locked loop (PLL) is implemented. This PLL continuously tracks the phase of the grid voltage. The phase (ωt) of the grid voltage, obtained from the PLL, is essential for implementing the dq transformation and inverse transformation.

2.6 Current Controller

The objective of the current control loop in this control scheme is to generate a reference voltage waveform for the inverter that meets the power demands specified by the outer power control loop [11]. Applying Kirchhoff's laws to the circuit, we obtain equation (1):

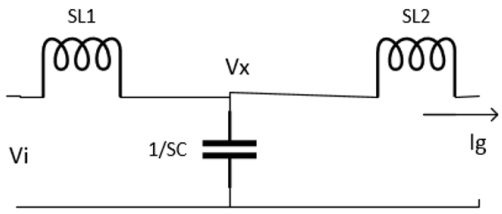

Figure 6: Circuit

$$L\frac{di}{dt} + Ri = V_i - V \tag{3}$$

Here, L = L1 + L2 and R = R1 + R2. In this simplification, the effect of the shunt capacitor is neglected as it offers much higher impedance to currents at the fundamental frequency. The inductance can be considered as connected in series. Vi denotes the inverter output voltage, V denotes the grid side voltage, and i denotes the grid injected current. Applying the dq transformation to Vi, i, V, we obtain equations:

$$L\frac{di}{dt} + R_{id} - \omega L_{iq} = V_{d1} - V_d \tag{4}$$

$$L\frac{di}{dt} + R_{iq} + \omega L_{id} = V_{q1} - V_q \tag{5}$$

As seen in equations (2) and (3), the d-axis and q-axis output currents are mutually dependent on each other. This leads to the need for complex control strategies unless these two are decoupled. These currents also depend on the grid voltage. In case of a grid disturbance, it will directly affect the system performance. To address these problems, the output reference voltage waveform used to generate the PWM switching is modified as follows. Let the reference output voltage components in the dq frame be represented as Vd1* and Vq1*. They are given as follows:

$$Vd1^* = Vd1 + \omega Liq - Vd \tag{6}$$

$$Vq1^* = Vd1 - \omega Liq - Vq \tag{7}$$

And hence,

$$L\frac{di}{dt} + Ri_d = Vd1^* \tag{8}$$

$$L\frac{di}{dt} + Ri_q = Vq1^* \tag{9}$$

By selecting the current control loop output to be V_{d1}^* and V_{q1}^*, we can observe that the i_d and i_q components will only depend on the inverter output voltage reference signal components. After generating these two components V_{q1}^* and V_{d1}^*, we can perform the inverse dq transformation and obtain the required reference signal to generate PWM pulses.

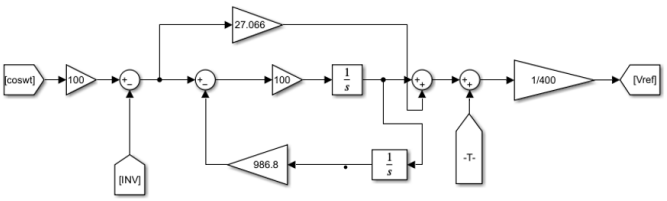

Figure 7: Current Controller

2.7 PWM Generator

To implement unipolar pulse width modulation, we need two sinusoidal reference signals. These signals should have the same amplitude and frequency, but they should be 180° out of phase with each other. These signals are then compared with a triangular carrier waveform to produce two pulse width modulation (PWM) signals.These two PWM signals are used to control the upper left and upper right switches of a full bridge circuit, while their inverse signals control the lower left and lower right switches. It's crucial to ensure that both switches on a single leg of the bridge are never turned on simultaneously.

If this were to happen, it would create a short circuit across the DC voltage source, which could lead to overcurrent and damage the switches.To prevent this, and to account for the switching characteristics of the insulated gate bipolar transistors (IGBTs) used in the circuit, a small delay or "dead band" is introduced between the switching on and off of the switches on the same leg. This ensures safe and efficient operation of the circuit. After generation of reference voltage from the controller, it is fed to the PWM generator and the carrier signal is adjusted. Unipolar modulation is used for which both positive and negative signal are used and comparators are used to compare reference signal and regenerating signal. Model of the PWM generator is designed;

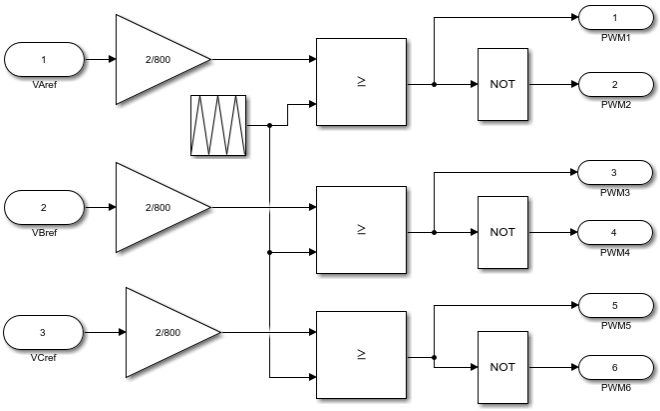

Figure 8: PWM generator

3. Simulation and Results

4.1 Model of Three-Phase Controller designed in MATLAB To validate the proposed system, a model is designed in MATLAB Simulink. The model includes an AC source representing the grid and a DC source connected to the system. An LCL filter is also incorporated into the model, along with all other necessary components. Two scenarios are examined in the simulation. The first scenario involved observing the flow of active power, while the second scenario focused on the flow of reactive power.

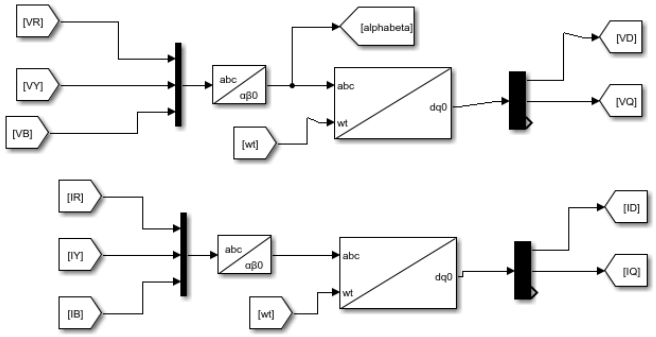

Figure 9: PLL

The model also includes a converter, which plays a crucial role in the system. The converter is responsible for transforming the DC power from the source into AC power compatible with the grid. It operates under the control of a sophisticated control scheme that ensures the quality of the power fed into the grid, minimizes harmonic distortion, and improves overall system performance.

The simulation results provide valuable insights into the system's performance under different conditions and validate the effectiveness of the proposed control scheme. These

results contribute to a better understanding of the dynamics of grid-connected DC power sources and inform the design of more efficient and reliable power systems [12]. Further analysis and discussion of the simulation results will be presented in the following sections.In order to conduct study of outer control strategy for active power control, following model is considered;

In the given system, an AC source with a voltage of 325 volts and a frequency of 50 Hz is connected to a DC voltage source of 400 volts through a converter. This converter implements the Synchronous Reference Frame Theory for control, and includes both a Phase-Locked Loop (PLL) and a current controller.

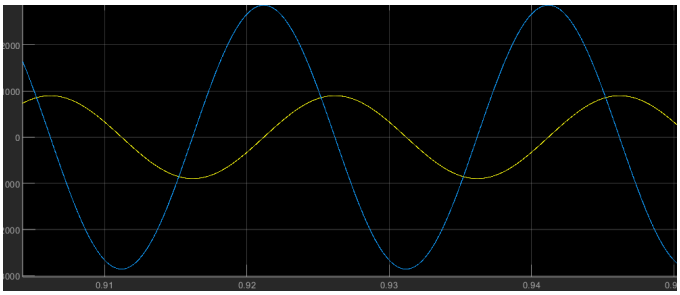

Figure 10: Reactive power control

The output of the grid voltage is obtained in such a way that it is in phase with the grid current. This implies that the system is operating under unity power factor conditions, which is highly desirable in power systems. Under these conditions, the real power and apparent power are equal, meaning that all the power supplied by the source is available for use in the load. This results in maximum power transfer and increased efficiency of the system.

Table 1: Parameters with Value used in MATLAB

S.N	Parameters	Value
1	Vdc	400Volt
2	Vgrid	230 Volt
3	P0	2kVA
4	Filter Capacitor	4.03microfarad
5	Grid Side Inductor	4.07mH
6	Inverter side Inductor	4.03mH
7	Switching Frequency	10kHz
8	Resonance Frequency	1416Hz
9	Irip	20%of rated current

The use of a converter with Synchronous Reference Frame Theory allows for better control of the power flow in the system. The PLL and current controller contribute to maintaining the stability of the system, ensuring that the voltage and current waveform are aligned, and that the current follows the reference current closely. This is crucial for the reliable and efficient operation of power systems, particularly in systems that integrate both AC and DC sources. Overall, this system demonstrates a sophisticated approach to managing and controlling power flow in a mixed AC/DC environment, leveraging advanced control theories and technologies to achieve optimal performance.

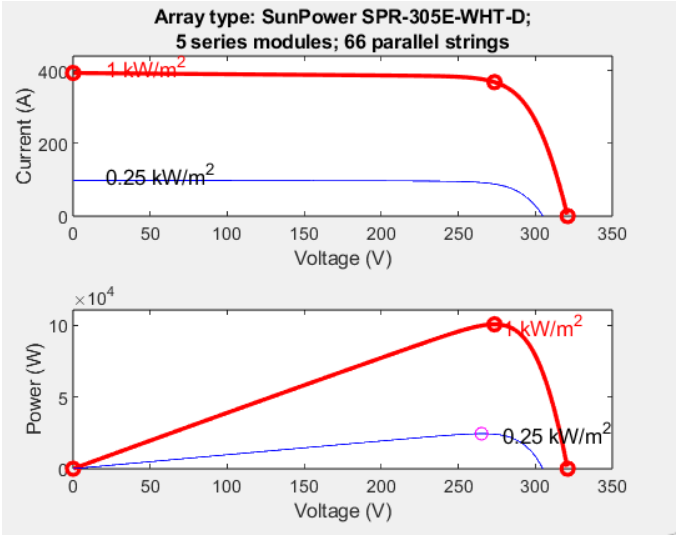

Figure 11: VI and PV curve of photovoltaic

After changing reference current to 5Amp it can be seen that there is phase difference grid voltage and grid current. Along with that there is phase difference between grid voltage and inverter current which shows flow of reactive power flow. Hence both active and reactive power flow are controlled by it successfully.

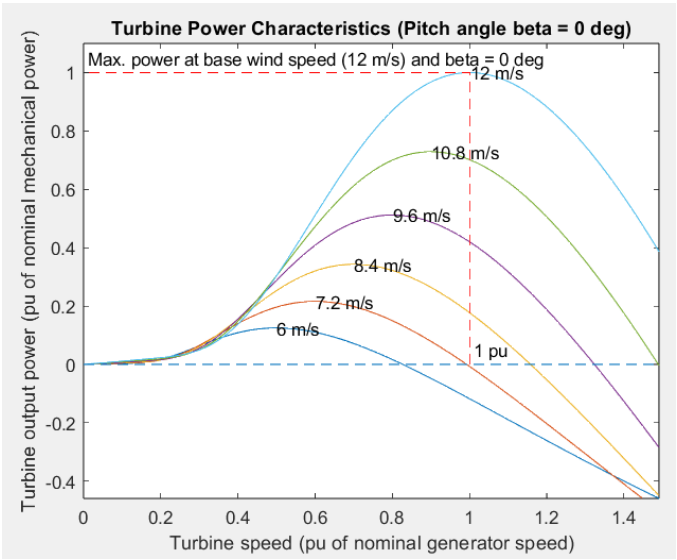

Figure 12: Output of wind generator

Furthermore, this in-phase condition indicates that the converter is effectively synchronizing the current it injects into the grid with the grid voltage. This synchronization is crucial for maintaining the stability and reliability of the power system.It also suggests that the control strategies implemented in the converter, such as the use of a Phase-Locked Loop (PLL) and current controller, are functioning effectively.

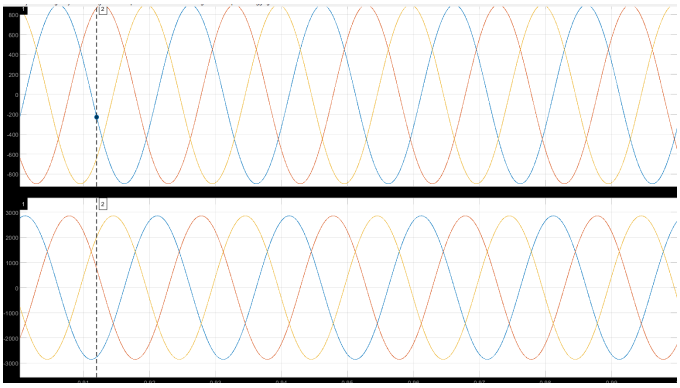

Figure 13: Active power with controller

4. Discussion

The discussion revolves around the integration of Direct Current (DC) sources into the existing Alternating Current (AC) grid, a critical step in meeting the rising demand for clean energy. The model proposed in this study is based on a single-phase system with an added DC source. A converter, designed using the synchronous reference frame, is introduced to address the challenges associated with integration. This converter enables the control of both active and reactive power using a dq reference frame, with a Proportional-Resonant (PR) controller employed for this purpose.

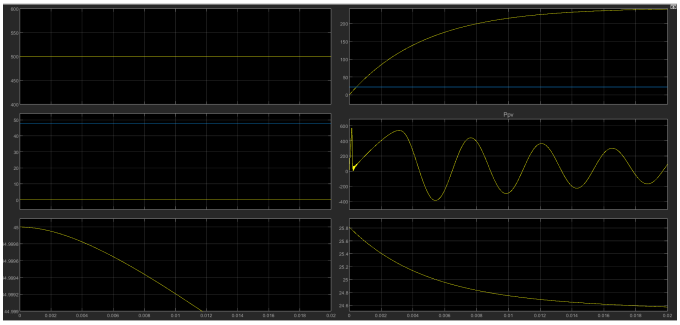

Figure 14: Output of Battery

The model also incorporates a Phase-Locked Loop (PLL) to generate the necessary operational references and an LCL filter known for its performance quality. The entire model is simulated in MATLAB, and the output obtained confirms the model's ability to control both active and reactive power when integrating DC with AC.

This work significantly contributes to efforts to integrate clean energy into existing grid systems. However, it's worth noting that while the model demonstrates control of both active and reactive power, further research and development are needed to optimize this control and address potential challenges in real-world applications. Future work could also explore the integration of other renewable energy sources and the use of advanced control strategies to enhance grid stability and reliability.

5. Conclusion

The total active load demand is 120 kW before 4 s, and each DG supply is 30 kW active power respectively. The ILC helps to transfer 20 kW from the AC to DC subgrid to realize the proportional power sharing of the microgrid. Meanwhile, each AC DG supplies is rated 10 kVar reactive power and the ILC transfers 20 kVar to the AC subgrid for the rated AC bus voltage. After 4 s, the AC and DC DGs supply is rated 80 kW active power respectively (40 kW each, as intended) and the ILC transfers 30 kW from the AC to DC subgrid. The active power supply of the AC and DC DGs increases to their rated values of 80 kW each after 4 seconds, as expected. To keep the proportional distribution of active power, the ILC moves 30 kW from the AC subgrid to the DC subgrid. Frequency regulation: In 4 seconds, the AC DGs' active power goes from 60 kW to their rated 80 kW. The AC frequency is impacted by this change in active power. The frequency shifts from 50.2 Hz to the specified 50 Hz, which highlights the droop characteristics' deviance. According to the text, compared to the conventional PI control, the disturbance suppression control approach efficiently lowers the transient frequency deviation. It can be concluded that proportional load demand sharing within the hybrid microgrid is realized. ILC in a hybrid AC/DC microgrid is presented, including Outer loop control strategy based on the flexible power sharing principle.

References

[1] Alexandru Baloi, Adrian Pana, and Florin Molnar-Matei. Advantages of using matlab simulink in laboratory lessons on operating conditions of overhead power lines. *Procedia - Social and Behavioral Sciences*, 191:179–184, 2015. The Proceedings of 6th World Conference on educational Sciences.

[2] Nepal Electricity Authority. *Annual Report*, 2023. Annual Progress of Fiscal year 79/80.

[3] Manoranjan Sahoo and K. Siva Kumar. Bidirectinal switched boost converter for ac-dc hybrid microgrid. *2014 IEEE Applied Power Electronics Conference and Exposition - APEC 2014*, pages 2231–2236, 2014.

[4] Farhad Shahnia, Ritwik Majumder, Arindam Ghosh, Gerard F. Ledwich, and Firuz Zare. Operation and control of a hybrid microgrid containing unbalanced and nonlinear loads. *Electric Power Systems Research*, 80:954–965, 2010.

[5] Hirofumi Akagi, Yoshihira Kanazawa, and Akira Nabae. Instantaneous reactive power compensators comprising switching devices without energy storage components. *IEEE Transactions on Industry Applications*, IA-20(3):625–630, 1984.

[6] Shamsher Ansari, Aseem Chandel, and Mohd. Tariq. A comprehensive review on power converters control and control strategies of ac/dc microgrid. *IEEE Access*, 9:17998–18015, 2021.

[7] Yanghong Xia, Yonggang Peng, Pengcheng Yang, Miao Yu, and Wei Wei. Distributed coordination control for multiple bidirectional power converters in a hybrid ac/dc microgrid. *IEEE Transactions on Power Electronics*, 32(6):4949–4959, 2017.

[8] Peng Wang, Chi Jin, Dexuan Zhu, Yi Tang, Poh Chiang Loh, and Fook Hoong Choo. Distributed control for

autonomous operation of a three-port ac/dc/ds hybrid microgrid. *I E E E Transactions on Industrial Electronics*, 62(2):1279 – 1290, February 2015.

[9] S. Golestan, J. M. Guerrero, and G. B. Gharehpetian. Five approaches to deal with problem of dc offset in phase-locked loop algorithms: design considerations and performance evaluations. *IEEE Transactions on Power Electronics*, 31:648–661, 2016.

[10] Joan Rocabert, Alvaro Luna, Frede Blaabjerg, and Pedro Rodriguez. Control of power converters in ac microgrids. *IEEE transactions on power electronics*, 27(11):4734–4749, 2012.

[11] Jessada Phan-on and Wirot Saengthongthong. Design equation for the gain of non-ideal resonance proportional controller used in controlling single-phase grid-connected inverter. *Srinakharinwirot University Engineering Journal*, 15(1):25–37, 2020.

[12] Frede Blaabjerg, Remus Teodorescu, Marco Liserre, and Adrian Vasile Timbus. Overview of control and grid synchronization for distributed power generation systems. *IEEE Transactions on Industrial Electronics*, 53(5):1398–1409, 2006.